Power Optimized DSTBC Assisted DMF Relaying in Wireless Sensor Networks with Redundant Super Nodes

Abolfazl Razi, Fatemeh Afghah, and Ali Abedi

Abstract—In conventional two-tiered Wireless Sensor Networks (WSN), sensors in each cluster transmit observed data to a fusion center via an intermediate supernode. This structure is vulnerable to supernode failure. A double supernode system model with a new coding scheme is proposed to monitor a binary data source. A Distributed Joint Source Channel Code (D-JSCC) is proposed for sensors inside a cluster that provides two advantages of low complexity transmitters and scalability to a large number of sensors.

In order to setup a robust communication channel from sensors to the data fusion center, Distributed Space-Time Block Coding (D-STBC) is employed at two supernodes prior to relaying that results in additional diversity gain. DeModulate and Forward (DMF) relaying mode is chosen to enable packet reformatting at the supernodes, which is not possible in widely used Amplify and Forward (AF) mode. The optimum power allocation for the two-hop multiple DMF relaying is calculated to minimize the system Bit Error Rate (BER). An upper bound is derived for the system end-to-end BER by analyzing a basic decoder operation over the system model. The simulation results validate this upper bound and also demonstrate considerable improvement in the system BER for the proposed coding scheme.

Index Terms—Distributed coding, demodulate and forward relaying, distributed space-time block codes, power optimization.

I. INTRODUCTION

CLASSICAL Wireless Sensor Network (WSN) solutions with direct data observation are not capable of addressing various practical harsh environmental and non-invasive applications. Some examples include: jet engine temperature monitoring, crack and corrosion detection in composite materials, and non-invasive biomedical diagnostics. In all these applications, the source of data is indirectly observed by several remote observer agents. Due to power constraint of tiny observer sensors, the collected data should be transmitted via an intermediate relay node to the data fusion center for subsequent data processing. Finding the optimum transmission technique for these situations considering the implementation constraints is still a challenging problem in WSN.

The indirect multi-terminal observation is first investigated by Berger et al introducing a model called Chief Executive Officer (CEO) [1]. This problem is intensively investigated from information theoretic perspective and rate distortion regions are found for some special cases including quadratic Gaussian case [2], [3]. Recently, several attempts are made to generalize the distortion rate regions and corresponding bounds to more generalized observation models [4], [5]. These theoretical limits are based on simplifying assumptions of unlimited number of observers and very large data block lengths. In this article, we examine this problem from a practical standpoint and propose a reliable and efficient coding scheme for limited number of sensors to estimate a binary data source.

In a traditional statically clustered two-tiered WSN, a supernode collects data from sensors inside a cluster and relays it to a data fusion center using different relaying modes [6]. This structure is not efficient and is vulnerable to supernode failure. To overcome this drawback and improve the system BER performance, a new system model based on using two supernodes at each cluster is proposed in this paper.

The first tier is composed of sensors in one cluster monitoring a binary data source. Noting the high correlation among sensors' data, overall system data flow efficiency can be considerably improved using Distributed Joint Source Channel Coding (D-JSCC) [7]–[9]. Most reported D-JSCC schemes are based on capacity achieving Low Density Parity Check (LDPC) and turbo codes that are too complex for computationally constrained sensors. The decoding complexity is almost impractical for a large number of sensors [10]–[14]. A practical low complexity D-JSCC solution based on a distributed version of Parallel Concatenated Convolutional Codes (PCCC) is introduced by authors in [15], which is applied to the first tier of the proposed system structure in the current work to enhance the end-to-end system error rate.

The second tier is composed of links from the supernodes to the base station. De-Modulate and Forward (DMF) relaying is applied to supernodes to enable reformatting of the received packets into a single multi-frame before forwarding to the base station. Distributed Space Time lock Codes (D-STBC) are widely used as a diversity technique in wireless networks [16]–[20]. In the proposed system model, the two supernodes is placed far apart, hence D-STBC can be employed prior to relaying to provide an additional diversity gain.

It is shown that for a multi-relay system with D-STBC assisted AF relaying, the optimum power allocation among source and relay nodes is equal power allocation [21]. BER performance for these systems with equal power allocation is analyzed in [22]. Surprisingly, the optimum power allocation for DMF relaying mode, found in this research, is not the equal power allocation.

The rest of this paper is organized as follows. The proposed two-tiered system model along with the coding scheme proposed for each tier are elaborated in section II. Section III includes analytical methods for power optimization and BER performance analysis. These results are verified by simulations in section IV. Concluding remarks are provided in section V.

II. System Model

The proposed two-tiered structure is depicted in Fig. 1. Each cluster includes a binary source observed by a group of sensors that form the first tier of the system. The optimum number of sensors in each cluster, M depends on the system quality conditions such as sensors' observation accuracy, channel SNR, and coding rate, which is discussed in [15]. The source data of different clusters assumed to be uncorrelated. There is no overlap between the clusters, hence we focus on one cluster, in this paper. The channels from sensors to the supernodes are orthogonal either in time or frequency. Both supernodes listen to the same channel set and receive different versions of the same signal.

The second tier is composed of two supernodes per cluster that forward the received signals from sensors to the base station using a method explained in section II-D. All channel coefficients are assumed to be independent Zero-Mean Complex Gaussian Random Variables (ZMCGRV). In summary, the system includes low complexity short range sensors, medium complexity supernodes and a computationally-rich base station which performs joint decoding and data fusion.

A. Binary Source Observation

In some applications, the observation accuracy is modeled as a joint Gaussian distribution for source and sensor measurement. This model is not usually realistic due to wide category of parameters under measurement including light, temperature, humidity, stress, pressure, etc. Moreover, the distortion from source to the sensors may be different than a Gaussian model. An approximate approach is to model the bit flipping between the digitized versions of the source data and observed data with a virtual BSC channel [12], [23]–[25]. The crossover probability of BSC channel from the source to the ith sensor, β_i, is the lower bound on the probability of bit flipping due to observation imperfectness.

Noting the above justification, we consider the source data $\mathbf{s} = \{s^1, s^2, ..., s^N\}$ as an independent identically distributed (i.i.d) equiprobable Bernoulli sequence of length N. The observation of sensor i is $\mathbf{s}_i = \{s_i^1, s_i^2, ..., s_i^N\}$, where $s_i^k = s^k \oplus e_i^k$. The term e_i^k is the observation error in the kth bit of $\mathbf{s}_i$ with probability $p(e_i^k = 1) = 1 - p(e_i^k = 0) = \beta_i$. For the sake of simplicity, equal observation accuracy is assumed for all sensors, $\beta_i = \beta$. Considering discrete memoryless channels
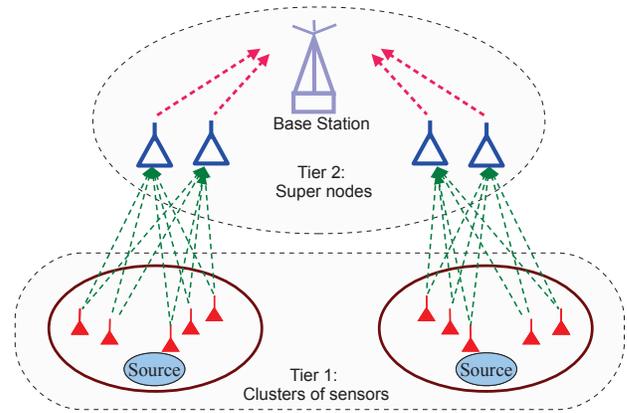
Fig. 1. System model for two-tiered double-sink wireless sensor network.
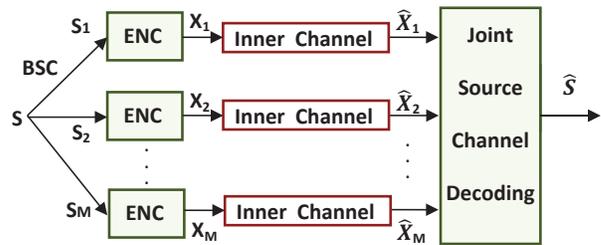
Fig. 2. Distributed joint source channel coding for cluster of sensors with correlated data. The two-hop multiple relay channels from the sensors to the base station is modeled as *inner channels*.

(DMC) and independent observation errors, the pairwise correlation between two sensors can also be modeled as a virtual BSC channel with crossover probability $\beta * \beta = 2\beta(1 - \beta)$. This fact is used in the iterative decoder implementation to estimate and use the correlation parameter at the receiver.

B. Encoder and Decoder Structures

In the proposed coding scheme to performs D-JSCC, each sensor node consists of a random interleaver followed by a RSC encoder. Feed forward and feedback polynomials of RSC encoders are arbitrarily set to $f(D) = 1 + D^2$ and $g(D) = 1 + D + D^2$, respectively. Parity and systematic bits are punctured using an appropriate pattern to form an output frame for the ith sensor $\mathbf{c}_i = \{c_i^1, c_i^2, ..., c_i^{N/R_c}\}$, where R_c is the desired coding rate per sensor. The resulting frame is BPSK modulated to form the output signal $\mathbf{x}_i = \{x_i^1, x_i^2, ..., x_i^{N/R_c}\}$. The output of all sensors, altogether form a distributed structure of PCCC. Since the orthogonal channels achieve the maximum sum rate of a multiple access channel [26], the frames are sent via orthogonal channels to the fusion center. The communication channel set from each sensor to the fusion center is called *inner channel* as depicted in Fig. 2 with details elaborated in section II-D.

Inspired by the encoder structure, a decoder based on Multiple Turbo Decoder (MTD) is used to decode the received frames and estimate the source bits. The block diagram of this decoder is presented in Fig. 3. The main idea is using other sensors' observations as side info in decoding any sensor's observation. Several modifications are applied to the
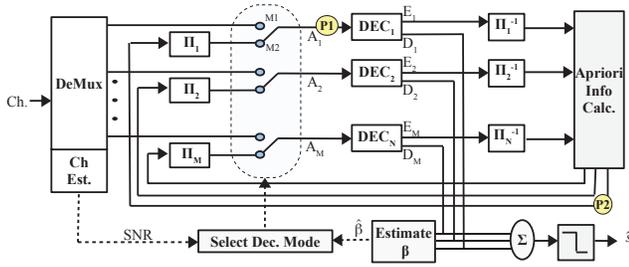
Fig. 3.   Iterative decoder based on MTD employed at the base station.

Fig. 4.   Channel coefficients for the communication links from sensors to the base station via two supernodes.

decoding algorithm including i) decoder initialization, ii) LLR exchange, iii) hard limiter and iv) iteration termination criterion in order to improve the performance of the MTD decoder. The modifications are based on the fact that despite traditional turbo decoder, the parity bits of each constituent decoder correspond to a particular sensor's observations, which are corrupted versions of a common data source. The observation accuracy of the sensors are not known at the receiver and can be adaptively extracted from the received frames. Details of the decoding algorithm is presented in [15].

C. Relaying Mode

Two supernodes at each cluster collect data from sensors and forward it to a data fusion center at the base station. Despite commonly used single supernode structure, we utilize two supernodes to make the system robust to supernode failure. This moreover, provides space diversity gain as analyzed in section III. Different relying modes can be used in supernodes. It has been shown that for orthogonal half duplex transmission with duty cycle of $1/2$, Decode and Forward (DF) mode outperforms AF and DMF modes if the channels from the source to relay are less noisy than the channels from relays to destination; otherwise the performance is almost similar [27]. In this paper we assume equal noise levels at two hops of the communications. However, we use DMF relaying because of the following reasons:

- Decoding complexity is proportional to the number of sensors and it is preferred to skip decoding at the medium-complexity relay nodes if not necessary (DF is not desired).
- Simulation results show lower performance for DF mode when the observation accuracy of sensors are low. Since by decoding at the relay nodes, some useful correlation information are lost at the destination.
- The performance of AF and DMF modes are almost equal. However, DMF mode is chosen in this work, since it enables packet reformatting at relay nodes. Different frames received from the sensors over orthogonal radio channels are put together to form a single multi-frame and forward to the base station over a single radio channel.

To obtain time diversity in addition to space diversity of order 2, when the channel coherence time is relatively small with respect to symbol duration, a distributed version of space time block codes (D-STBC) is employed at the relay nodes, as presented in sections II-D and IV.
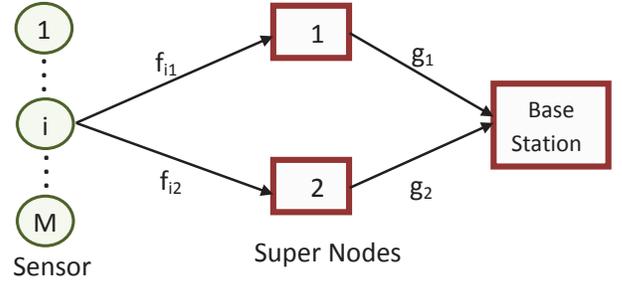
D. Inner Channel Model

The so called *inner channels* from each sensor to the base station form a multi-relay structure as depicted in Fig. 4. The *inner channel* corresponding to the ith sensor, consists of two fading channel sets f_{ij} and g_j, where f_{ij} represents the channel coefficient between sensor i ($i \in \{1, \dots, M\}$) and supernode j ($j \in \{1, 2\}$) and g_j represents the channel coefficient between supernode j and the base station. The channel coefficients are i.i.d ZMCGRV, $f_{ij}, g_j \sim \mathcal{CN}(0, 1)$. The channel information, f_{ij} and g_i are assumed to be known only at the receiver, enabling the use of coherent detection. To model a communication link from one arbitrary sensor to the base station, we will omit the index i in f_{ij} and use f_j, hereafter.

In a $R \times D$ D-STBC scheme, K consecutive symbols are sent over R transmit antennas using orthogonal $R \times K$ matrices, where D is the number of receive antennas at the destination. The normalized transmit data of an arbitrary sensor is presented by $(\mathbf{x})_{K \times 1} = [x^1 \ x^2 \ \dots x^K]^T$ such that $E\{\mathbf{xx}^*\} = T$, where E(.) is expected value function and $(.)^T$ and $(.)^*$ denote transpose and conjugate transpose operations, respectively. For 2×1 STBC used in the proposed model, we have $R = K = 2, D = 1$.

If P_1 is the power assigned to each sensor, the received signal at the jth supernode during two consecutive time intervals is

$$\mathbf{r_j} = \sqrt{P_1} f_j \mathbf{x}_i + \mathbf{v_j} \ , \ j = 1, 2 \qquad (1)$$

where $\mathbf{v_j}$ is a 2×1 noise vector whose elements are ZMCGRV with variance of N_1. Coherent symbol by symbol maximum likelihood detection (MLD) is performed to calculate demodulated packet $\hat{\mathbf{x}}_j = [x_j^1, x_j^2, \dots x_j^K]^T$ as

$$\hat{x}_j^k = \underset{x \in \mathcal{X}}{arg \ min} \left| x - \frac{r_j^k}{\sqrt{P_1} f_j} \right| \qquad (2)$$

where $\mathcal{X}$ is the constellation map.

The error vector is $\mathbf{e}_j = \hat{\mathbf{x}}_j - \mathbf{x} \in \mathcal{E}^T$, where $\mathcal{E} = \{x_i - x_j : \ \forall x_i, x_j \in \mathcal{X}\}$ is the error support set. For BPSK modulation, we have $\mathcal{X} = \{-1, 1\}$ and $\mathcal{E} = \{0, 2, -2\}$.

The resulting symbols are space-time coded and transmitted

to the base station as follows,

$$\mathbf{t_j} = \mathbf{A_j}\hat{\mathbf{x}}_j + \mathbf{B_j}\bar{\hat{\mathbf{x}}}_j \tag{3}$$

where $\bar{\mathbf{x}}_j$ denotes the conjugate of vector $\mathbf{x}_j$. $\mathbf{A_j}$ and $\mathbf{B_j}$ are $R \times K$ real and imaginary unitary STBC matrices. For 2×1 D-STBC with real-valued BPSK modulation, following [28] they are chosen as

$$\mathbf{A_1} = \begin{pmatrix} 1 & 0 \\ 0 & -1 \end{pmatrix}, \mathbf{A_2} = \begin{pmatrix} 0 & 1 \\ 1 & 0 \end{pmatrix}, \mathbf{B_1} = \mathbf{B_2} = \mathbf{0}. \tag{4}$$

Therefore, the received signal, $\mathbf{y} = [y^1 \ y^2]^T$ at the base station is

$$\begin{aligned} \mathbf{y} &= \sum_{j=1}^{2} g_j \sqrt{P_{2j}} \mathbf{A_j}\hat{\mathbf{x}}_j + \mathbf{w} \\ &= \sum_{j=1}^{2} g_j \sqrt{P_{2j}} \mathbf{A_j}\mathbf{x}_j + \sum_{j=1}^{2} g_j \sqrt{P_{2j}} \mathbf{A_j}\mathbf{e}_j + \mathbf{w} \end{aligned} \tag{5}$$

where $\mathbf{w}$ is a 2×1 random vector whose elements are ZMCGRV with variance N_2 and P_{2j} is transmit power of relay node j such that $P_{21} = P_{22} = \frac{P_2}{2}$.

III. PERFORMANCE ANALYSIS

In order to analyze the system BER performance, we first calculate the probability of error for the *inner channels*. Then, we derive an upper bound on the whole system end-to-end BER performance.

In the proposed scheme, sensors transmit through orthogonal carriers, hence there is no need for time synchronization among sensors. The relay nodes do not need channel state information (CSI). We only need full CSI at the destination, which can be obtained using training sequences in practical applications. Therefore, a symbol based synchronization is required at relays similar to [21], which is more practical than carrier-level synchronization assumed in [29] and [30]. This level of synchronization can be easily implemented in moderate-complexity supernodes. For continuous data transmission, this can be achieved by instant relaying, since the radio paths are very short and do not adversely affect time synchronization.

A. Inner Channel BER Performance

The probability of error for Rayleigh fading channels from sensors to supernodes $p_e^{(sr)}$, for coherent detection in equation (2), can be calculated as in [31],

$$\begin{aligned} p_e^{(sr)} &= E_{f_j}\left\{Q\left(\sqrt{2|f_j|^2\gamma_1}\right)\right\} = \frac{1}{2}\left(1 - \sqrt{\frac{\gamma_1}{\gamma_1 + 1}}\right) \\ &\approx \frac{1}{4(\gamma_1 + 1)}, \quad \gamma_1 \to \infty \end{aligned} \tag{6}$$

where $\gamma_1 = \frac{P_1}{N_1}$ is the average SNR of the supernodes; $E_x(.)$ is expected value respect to x.

For DMF relaying and BPSK modulation, the error vector at the jth sink, $\mathbf{e}_j = [e_j^1 \ e_j^2]^T$ has the following pdf:

$$p(e_j^k = l) = \begin{cases} 1 - p_e^{(sr)} & l = 0 \\ p_e^{(sr)} & l = -2x_i \end{cases} \tag{7}$$

Considering full CSI at the receiver and the orthogonality of unitary matrices A_j, it can be shown that the detection problem reduces to the following Gaussian scalar detection problem:

$$\begin{aligned} \hat{x}_1 &= \arg\min_{x \in \mathcal{X}}\left|x - \frac{\bar{g}_1 y_1 + g_2 \bar{y}_2}{\sqrt{P_2/2} \parallel \mathbf{g} \parallel^2}\right| \\ \hat{x}_2 &= \arg\min_{x \in \mathcal{X}}\left|x - \frac{\bar{g}_2 y_1 - g_1 \bar{y}_2}{\sqrt{P_2/2} \parallel \mathbf{g} \parallel^2}\right| \end{aligned} \tag{8}$$

where $\parallel . \parallel$ is Frobenius norm and $\mathbf{g} = [g_1 \ g_2]$ is the channel vector from supernodes to the base station. Using (5), equation set (8) can be rewritten as

$$\begin{aligned} \hat{x}_1 &= \arg\min_{x \in \mathcal{X}}\left|\sqrt{P_2/2} \parallel \mathbf{g} \parallel (x - x_1) + n_1\right| \\ \hat{x}_2 &= \arg\min_{x \in \mathcal{X}}\left|\sqrt{P_2/2} \parallel \mathbf{g} \parallel (x - x_2) + n_2\right| \end{aligned} \tag{9}$$

where noise terms n_1 and n_2 can be decomposed into three terms. For instance, n_1 is

$$n_1 = \underbrace{\frac{\bar{g}_1 w_1 + g_2 \bar{w}_2}{\parallel \mathbf{g} \parallel}}_{n_{11}} + \underbrace{\frac{\bar{g}_1 g_2(e_2^2 - e_1^2)}{\parallel \mathbf{g} \parallel}\sqrt{P_2/2}}_{n_{12}} + \underbrace{\frac{|g_1|^2 e_1^1 + |g_2|^2 e_2^1}{\parallel \mathbf{g} \parallel}\sqrt{P_2/2}}_{n_{13}}. \tag{10}$$

Term n_{11} is a ZMCGRV with variance N_2, since a Gaussian random vector with covariance matrix proportional to the identity matrix preserves its distribution after multiplication by a unitary matrix. Terms n_{12} is a zero mean discrete RV with variance

$$\begin{aligned} E[n_{12}^2] &= E[\frac{|g_1 g_2|^2(e_2^2 - e_1^2)^2 P_2}{2 \parallel \mathbf{g} \parallel^2}] \\ &\overset{(a)}{=} \frac{P_2}{2}E[(e_2^2 - e_1^2)^2]E[\frac{|g_1 g_2|^2}{|g_1|^2 + |g_2|^2}] \\ &\overset{(b)}{=} 4P_2 p_e^{(sr)}(1 - p_e^{(sr)})E[\frac{|g_1 g_2|^2}{|g_1|^2 + |g_2|^2}] \\ &\overset{(c)}{=} \frac{4}{3}P_2 p_e^{(sr)}(1 - p_e^{(sr)}) \end{aligned} \tag{11}$$

where (a) follows from the independence of noise terms e_j^k and channel coefficients g_j; (b) follows directly from equation (7) and independence of e_j^k RVs; and (c) follows from the following proposition.

Proposition 1: If g_1 and g_2 are independent unit variance ZMCGRVs, then $E[\frac{|g_1 g_2|^2}{|g_1|^2 + |g_2|^2}] = \frac{1}{3}$.

Proof: We note that $|g_j|$ is a Rayleigh distributed RV with pdf $f(g_j) = \frac{g_j}{\sigma_g^2}e^{-\frac{g_j^2}{2\sigma_g^2}}$, where $\sigma_g^2 = 0.5$ is the variance of real and imaginary parts of g_j, hence we have

$$\begin{aligned} I_1 &= E\left(\frac{|g_1 g_2|^2}{|g_1|^2 + |g_2|^2}\right) \\ &= \int_0^\infty \int_0^\infty \frac{|g_1 g_2|^2}{|g_1|^2 + |g_2|^2} \cdot \frac{g_1 g_2}{\sigma_g^4}e^{-\frac{g_1^2 + g_2^2}{2\sigma_g^2}} dg_1 dg_2. \end{aligned} \tag{12}$$

Change of variables to polar format $(g_1, g_2) \sim (r\cos\theta, r\sin\theta)$ yields

$$I_1 = 4\int_{r=0}^{\infty}\int_{\theta=0}^{\frac{\pi}{2}} r^5 \sin^3\theta\cos^3\theta e^{-r^2} d\theta dr$$
$$= 4\Big(\int_0^{\infty} r^5 e^{-r^2} dr\Big)\Big(\int_0^{\frac{\pi}{2}} \frac{\sin^3 2\theta}{8} d\theta\Big) = 4(1)(\frac{1}{12}) = \frac{1}{3}. \tag{13}$$

This completes the proof. ∎

Thus, n_{12} is a zero-mean noise term with variance $\frac{4}{3}P_2 p_e^{(sr)}(1-p_e^{(sr)})$. It is a well-known fact that the Gaussian distribution maximizes the entropy of a RV with a given variance, hence Gaussian noise is the most unpredictable and hence the most harmful noise in a point to point communication [26], [32]. Recently, it is shown that Gaussian noise is the worst-case additive noise in general [26], [33]. Therefore, it is reasonable to conservatively model an arbitrary noise term with an equivalent Gaussian noise of the same variance. We do so for n_{12}.

In order to be more accurate, we plot the distribution of this noise term in Fig. 5. We observe that the resulting distribution, in fact is very close to a Gaussian distribution with an impulse response at origin. The impulse response is due to the probability of $p(e_2^2 - e_1^2 = 0)(p_e^{(sr)})^2 + (1-p_e^{(sr)})^2$. The Gaussian approximation of the noise term n_{12} with and without considering the impulse at the origin is represented in this figure by Approx. 1 and Approx. 2, respectively. Approximation 2 is more accurate but it needs conditional treating by considering only the case of $p(e_2^2 - e_1^2 \neq 0)$. However, the simulation results demonstrate negligible difference in the inner channel end-to-end error probability for the two approximations. Therefore, we use the pure Gaussian Approximation 1 for the sake of simplicity in the resulting equations. It is noteworthy that we checked the validity of both approximations using Kolmogorov-Smirnov test for goodness of fit [34], [35]. Empirical distribution of n_{12} obtained from both approximations using 10000 points pass this test. The test result confirms that we can assume that the samples of n_{12} are derived from a Gaussian noise with deviation less than 5% from the pdf [34], [35]. Therefore, n_{11} and n_{12} altogether, may be modeled as a ZMCGRV with variance $N_2' = N_2 + \frac{4}{3}p_e^{(sr)}(1-p_e^{(sr)})P_{21}$.

The discrete noise term n_{13} takes 4 values based on e_1^1 and e_2^1. According to (7) and (10) we have the following pdf for n_{13}

$$p(n_{i3} = l) = \begin{cases} (1-p_e^{(sr)})^2 & l = 0 \\ (1-p_e^{(sr)})p_e^{(sr)} & l = -2\frac{|g_2|^2}{\|\mathbf{g}\|}x_i\sqrt{P_2/2} \\ p_e^{(sr)}(1-p_e^{(sr)}) & l = -2\frac{|g_1|^2}{\|\mathbf{g}\|}x_i\sqrt{P_2/2} \\ (p_e^{(sr)})^2 & l = -2\|\mathbf{g}\|x_i\sqrt{P_2/2}. \end{cases} \tag{14}$$

This noise term intends to move the mean of the scaled received signal from $(x_i\sqrt{P_2/2})$ towards $(-x_i\sqrt{P_2/2})$ that increases the error probability. To quantify the effect of this term, for a given x_i value, we note that

$$E_g(n_i) = E_g(n_{i1}) + E_g(n_{i2}) + E_g(n_{i3}) = E_g(n_{i3}). \tag{15}$$
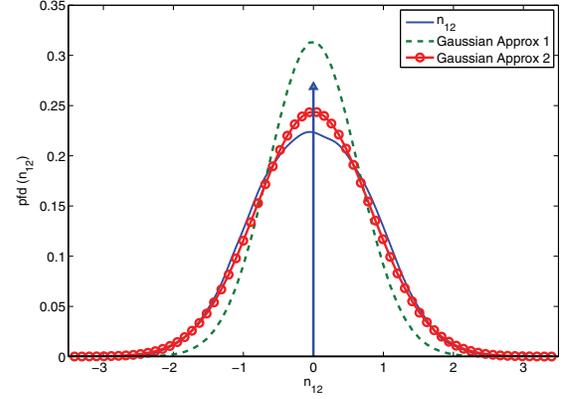
Fig. 5. Probability distribution function of noise term n_{12} and its approximation with Gaussian distribution. $p_e^{(sr)} = 0.1$ and $\sigma_{g_1} = \sigma_{g_2} = 1$.

It immediately follows that

$$p(E[\sqrt{P_2/2}\|\mathbf{g}\|x_i + n_i] = l) =$$
$$\begin{cases} (1-p_e^{(sr)})^2 & l = \|\mathbf{g}\|x_i\sqrt{P_2/2} \\ (1-p_e^{(sr)})p_e^{(sr)} & l = \frac{(|g_1|^2-|g_2|^2)}{\|\mathbf{g}\|}x_i\sqrt{P_2/2} \\ p_e^{(sr)}(1-p_e^{(sr)}) & l = \frac{(-|g_1|^2+|g_2|^2)}{\|\mathbf{g}\|}x_i\sqrt{P_2/2} \\ (p_e^{(sr)})^2 & l = -\|\mathbf{g}\|x_i\sqrt{P_2/2}. \end{cases} \tag{16}$$

To summarize, considering noise term n_{13} as a shift in the signal mean value and treating $n_{11} + n_{12}$ as a Gaussian noise term with variance N', the overall probability of inner channel error, $p_e^{(in)}$, can be calculated as

$$p_e^{(in)} = \sum_{n_{i3}} p(n_{i3})p^{(in)}(error|n_{i3})$$
$$= (1-p_e^{(sr)})^2 E_{\mathbf{g}}\Big[Q\Big(\sqrt{\|\mathbf{g}\|^2 \gamma_2}\Big)\Big]$$
$$+ (p_e^{(sr)})^2 E_{\mathbf{g}}\Big[Q\Big(-\sqrt{\|\mathbf{g}\|^2 \gamma_2}\Big)\Big]$$
$$+ 2p_e^{(sr)}(1-p_e^{(sr)})E_{\mathbf{g}}\Big[Q\Big(\frac{|g_1|^2-|g_2|^2}{\|\mathbf{g}\|}\sqrt{\gamma_2}\Big)\Big] \tag{17}$$

where $p^{(in)}(error|n_{i3})$ is the probability of error for a given n_{i3} value, and $\gamma_2 = \frac{P_2}{N_2'}$ is the average equivalent SNR at the base station. To calculate the above expression we have used the following proposition.

Proposition 2: Let $\mathbf{g} = [g_1 \ g_2]$ is a vector with ZMCGRV elements and c is a scalar value, then we have $E_{\mathbf{g}}[Q(\frac{|g_1|^2-|g_2|^2}{\|\mathbf{g}\|}c)] = \frac{1}{2}$.

Proof: By symmetry, we note that $x = \frac{|g_1|^2-|g_2|^2}{\|\mathbf{g}\|}c$ is a RV with even pdf, $f(-x)=f(x)$. Noting $Q(-x) = 1 - Q(x)$, it

results

$$E[Q(x)] = \int_{-\infty}^{\infty} Q(x)f(x)dx$$
$$= \int_{-\infty}^{0} Q(x)f(x)dx + \int_{0}^{\infty} Q(x)f(x)dx$$
$$= \int_{0}^{\infty} (1 - Q(x))f(x)dx + \int_{0}^{\infty} Q(x)f(x)dx$$
$$= \int_{0}^{\infty} f(x)dx = \frac{1}{2}. \tag{18}$$

This completes the proof. ∎

Considering proposition 2, equation (17) is simplified to

$$p_e^{(in)} = p_e^{(sr)} + p_e^{(rd)} - 2p_e^{(sr)}p_e^{(rd)} \tag{19}$$

where $p_e^{(rd)}$ is

$$p_e^{(rd)} = E_{\mathbf{g}}\Big[Q\Big(\sqrt{\| \mathbf{g} \|^2 \gamma_2}\Big)\Big]. \tag{20}$$

To calculate $p_e^{(rd)}$, we note that the channel coefficients g_i are ZMCGRVs, hence $\| \mathbf{g} \|^2$ is a Chi-square distributed RV with 4 degrees of freedom. It is shown in [31] that equation (20) for a Chi-square RV with $2L$ degrees of freedom can be written as

$$p_e^{(rd)} = \Big(\frac{1}{2} - \frac{1}{2}\sqrt{\frac{\gamma_2}{\gamma_2 + 2}}\Big)^L \times$$
$$\sum_{l=0}^{L-1} \binom{L-1+l}{l} \Big(\frac{1}{2} + \frac{1}{2}\sqrt{\frac{\gamma_2}{\gamma_2 + 2}}\Big)^l \tag{21}$$

where $\binom{n}{m} = \frac{n!}{m!(n-m)!}$. Setting $L = 2$ and using approximation $\sqrt{1+x} \approx 1 + \frac{1}{2}x$ for small x, (21) is simplified to

$$p_e^{(rd)} = \frac{1}{2}\Big(1 - \frac{\gamma_2 + 3}{\gamma_2 + 2}\sqrt{\frac{\gamma_2}{\gamma_2 + 2}}\Big)$$
$$\approx \frac{1}{2(\gamma_2 + 2)^2}, \quad \gamma_2 \to \infty. \tag{22}$$

Combining equations (6), (19), and (22) results in the following expression for the overall bit error probability:

$$p_e^{(in)} = \frac{1}{4(\gamma_1 + 1)} + \frac{1}{2(\gamma_2 + 2)^2} - \frac{1}{4(\gamma_1 + 1)(\gamma_2 + 2)^2} \tag{23}$$

which clearly is

$$p_e^{(in)} = p_e^{(sr)} * p_e^{(rd)} = p_e^{(sr)}(1 - p_e^{(rd)}) + (1 - p_e^{(sr)})p_e^{(rd)} \tag{24}$$

where $(*)$ denotes convolution operation. This resulting expression is interestingly equal to the error probability of cascade of two channels with error probabilities $p_e^{(sr)}$ and $p_e^{(rd)}$.

For simplicity, we assume equal noise power at relay and destination nodes $N_1 = N_2 = N$. Then, γ_1 and γ_2 can be calculated as follows,

$$\begin{cases} P_1 = \alpha P \\ P_2 = \bar{\alpha} P \\ \bar{\alpha} = 1 - \alpha \end{cases} \Rightarrow \begin{cases} \gamma_1 = \frac{P_1}{N_1} = \alpha\frac{P}{N} = \alpha\gamma \\ \gamma_2 = \frac{P_2}{N_2} = \frac{\bar{\alpha}P}{N + \frac{4}{3}p_e^{(sr)}(1 - p_e^{(sr)})\bar{\alpha}P} \end{cases} \tag{25}$$

where α is the portion of power allocated to the sensor nodes. Substituting the value of $p_e^{(sr)}$ in (6), γ_2 becomes

$$\gamma_2 = \frac{\bar{\alpha}P}{N + \frac{4}{3}p_e^{(sr)}(1 - p_e^{(sr)})\bar{\alpha}P}$$
$$\approx \frac{12\alpha^2\bar{\alpha}\gamma^2}{8\alpha^2\gamma + 4\alpha\gamma + \alpha - 1}$$
$$\approx \frac{3\alpha\bar{\alpha}\gamma}{2\alpha + 1}, \quad \gamma \to \infty. \tag{26}$$

Therefore, the equivalent SNR for the links from source to relay and from relay to destination, are both factors of the total SNR value as

$$\gamma_1 = \alpha\gamma,$$
$$\gamma_2 = \eta\gamma, \quad (\eta = \frac{3\alpha\bar{\alpha}}{2\alpha + 1}). \tag{27}$$

Substituting the above values of γ_1 and γ_2 into (23), it can be rewritten as

$$p_e^{(in)} = \frac{1}{4(\alpha\gamma + 1)} + \frac{1}{2(\eta\gamma + 2)^2} - \frac{1}{4(\alpha\gamma + 1)(\eta\gamma + 2)^2}. \tag{28}$$

It can be seen that when the total SNR approaches infinity, both γ_1 and γ_2 approach infinity and the first term $p_e^{(sr)} = \frac{1}{4(\alpha\gamma + 1)}$ is dominant. Hence, more power should be assigned to the source nodes to compensate this error as seen in the simulation results.

To analyze the two extreme cases of power allocation $\alpha = 0$ and $\alpha = 1$, we note that if we assign all the power to the second layer, $\alpha \to 0$, then $p_e^{(in)}$ saturates to about $\frac{1}{2}$ regardless of SNR value. This obviously is because no information is sent from the source to relay nodes. On the other hand, if $\alpha \to 1$ and consequently $\eta \to 0$, the same fact applies due to the high error rate in $p_e^{(rd)}$ for any SNR value. Consequently, α should be chosen carefully in range $(0, 1)$ considering the channel noise power. To optimize α, we note that the error probability $p_e^{(in)}$ in (28) is a convex function of α. To find the optimum power allocation, one can take derivative of (28) with respect to α and set it equal to zero. This also can be solved using numerical methods. The optimum power allocation parameter, for different $SNR = \frac{P}{N_1}$ values are presented in Table. I.

TABLE I
OPTIMUM POWER ALLOCATION FOR DIFFERENT SNR VALUES

SNR (dB)	10	15	20	25
α	0.65	0.71	0.78	0.84

It is noteworthy that we assumed equal noise levels and equal path losses for the two hops of communications (the channels from the source to relays and channels from relays to the destination). If we take into account the path loss of l for the first hop of the inner link, (1) changes to

$$\mathbf{r_j} = \sqrt{P_1}lf_j\mathbf{x}_i + \mathbf{v_j} \quad \Rightarrow \quad \mathbf{r_j}/l = \sqrt{P_1}f_j\mathbf{x}_i + \mathbf{v'_j}, \quad j = 1, 2 \tag{29}$$

which is equivalent to the original system with noise level divided by l. Thus, unequal noise levels case covers this effect as well. We assumed equal noise power at relays and

destination, so far, for the sake of simplicity. However, all the calculations hold for unequal noise levels as well. We only need to skip using relation $N_1 = N_2 = N$ from (25) and its subsequent equations. In Fig. 7, the optimum power allocation is shown for this general case.

B. Overall System BER Performance

The *inner channel* error probability $p_e^{(in)}$, derived in (28), is used in this section to analyze the system overall BER performance. To derive an upper bound on the system end-to-end BER performance, we consider a *basic decoder* operation over the *inner channel* as a reference system. The *basic decoder* consists of MAP decoders, each corresponding to a RSC encoder, followed by a symbol-by-symbol MLD. This decoder is obtained by setting the switch in position $M1$ and bypassing information exchange among constituent decoders in Fig. 3. Each constituent decoder performs decoding individually and provides estimations for the corresponding sensor's observations bits. Considering the equal sensor accuracies and symmetry of channels, MLD reduces to a majority vote rule. Majority vote is performed on the resulting hard bits to yield estimations of the source bits. The performance of this decoder is analyzed over the *inner channel*, which is replaced by an equivalent BSC channel with error probability $p_e^{(in)}$.

The bit Weight Enumeration Function (WEF) for the utilized RSC encoders with feed forward and feed back ploynomials $f(D) = 1 + D^2$ and $g(D) = 1 + D + D^2$, is calculated following the procedure in [36],

$$
\begin{aligned}
B(X) &= \frac{3X^5 - 6X^6 + 2X^7}{1 - 4X + 4X^2} \\
&= 3X^5 + 6X^6 + 14X^7 + 32X^8 + \ldots
\end{aligned}
\tag{30}
$$

which presents the weight spectrum of the RSC encoder. For instance, we have three code words with bit weight 5, six codewords with bit weight 6 and so on. An upper-bound on the bit error probability of a RSC encoder over a BSC channel with small crossover probability, $p_e^{(in)}$ according to [36] is

$$
p_e^{(rsc)} \le B(X)\big|_{X=2\sqrt{p_e^{(in)}\bar{p}_e^{(in)}}} \approx B_{dfree}\left(2\sqrt{p_e^{(in)}\bar{p}_e^{(in)}}\right)^{d_{free}}
\tag{31}
$$

where $d_{free} = 5$ is the minimum distance of the code and $B_{dfree} = 3$ is the coefficient of the corresponding term in $B(X)$.

The output bit of each RSC decoder may be in error either because of the corresponding sensor's observation error β_i or due to channel error $p_e^{(rsc)}$. Hence, the probability of bit error after RSC decoding with respect to the source signal is upper bounded by

$$
p_e^i \le \beta_i \otimes p_e^{(rsc)} = \beta_i(1 - p_e^{(rsc)}) + (1 - \beta_i)p_e^{(rsc)}.
\tag{32}
$$

The output of the RSC decoders are fed into the majority vote decoder, where the output bit is set to 0, if the value of the corresponding output bits at half or more of the decoders are 0, otherwise it is set to 1. Hence, a particular output bit is in error, if the corresponding bit in more than half of the sensors is decoded incorrectly. For even number of the sensors, if half of the bits decoded correctly then the output of ML detector

is in error with probability $\frac{1}{2}$. Consequently, the overall bit error probability of the system, is upper-bounded by

$$
p_e \le \begin{cases} \sum_{i=\frac{M+1}{2}}^{M} \binom{M}{i} p^i \bar{p}^{M-i} & \text{M is odd} \\ \sum_{i=\frac{M}{2}+1}^{M} \binom{M}{i} p^i \bar{p}^{M-i} + \frac{1}{2}\binom{M}{M/2} p^{M/2}\bar{p}^{M/2} & \text{M is even} \end{cases}
\tag{33}
$$

where we have $p = 1 - q = p_e^i$. The two above upper bound equations for odd and even number of sensors can be combined to the following expression:

$$
p_e \le \sum_{i=\lfloor \frac{M}{2} \rfloor + 1}^{M} \binom{M}{i} p^i q^{M-i} + \frac{(-1)^M + 1}{4}\binom{M}{\frac{M}{2}}(pq)^{\frac{M}{2}}
\tag{34}
$$

where $\lfloor . \rfloor$ denotes floor function. This is an upper bound on the probability of error in detecting a single bit of the source data using the proposed coding scheme over defined system model. This is plotted and compared to the simulation results of the proposed coding scheme in the next section.

It is notable that if we consider an error free channels from the sensors to the destination, we can replace p with β in (34),

$$
p_e^{floor} = \sum_{i=\lfloor \frac{M}{2} \rfloor + 1}^{M} \binom{M}{i} \beta^i \bar{\beta}^{M-i} + \frac{(-1)^M + 1}{4}\binom{M}{\frac{M}{2}}(\beta\bar{\beta})^{\frac{M}{2}}.
\tag{35}
$$

This is the lowest end-to-end error probability that can not be compensated by means of coding and appear as BER floor in Fig. 8. This error floor for low and moderate observation accuracies is often dominant to the error floor imposed by the decoding algorithm.

IV. SIMULATION RESULTS

In this section, the simulation results for the proposed system are presented. First, BER performance of the *inner channels* is analyzed. Then, the overall system end-to-end BER performance considering both communication layers is evaluated. In all simulations, data frames with 256 bits length, BPSK modulation, i.i.d equiprobable Bernoulli input bit stream, observation error of $\beta = 0.01$ and orthogonal Rayleigh distributed block fading channels are considered, except otherwise explicitly specified.

Fig. 6 presents the impact of power allocation on *inner channel* error probability. Despite STBC assisted AF-relaying, where the optimality achieved if the total power is equally divided between the two tiers (sensors and relays), the performance curve of DMF relaying mode is not symmetric. Dashed and solid lines in this figure presents analytical and simulation results for error probability as a function of power allocation parameter α. Simulation results match the analytical expression derived in (28), specially for large SNR values, where the approximations hold better. One interesting result is that allocating more power to the sensor nodes, specially at large SNR values improves the performance. The optimum power allocation scenario can be chosen based on the average SNR value of the system, $\frac{P}{N_1}$. The optimum power allocation
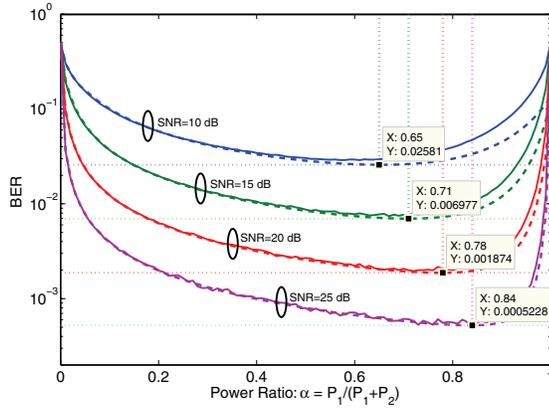
Fig. 6. Probability of error for *inner channels* versus power allocation parameter α.

Fig. 8. Probability of error for *inner channel* and the whole system, number of sensors: 4.

Fig. 7. Optimum power allocation vs SNR: $\frac{P}{N_1+N_2}$ for different noise levels.
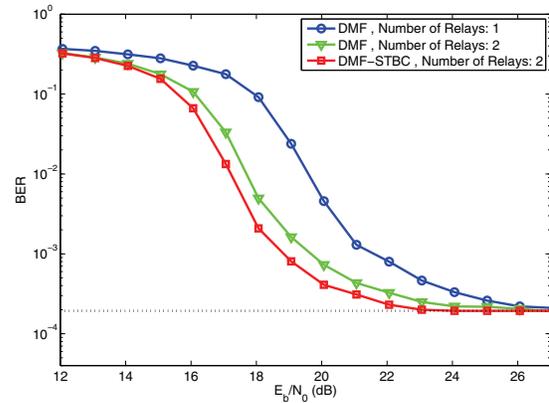
Fig. 9. Comparison of system performance for different number of supernodes, with and without STBC coding at supernodes, number of sensors: 4.

parameters for some SNR values that presented in Table I, are marked in this figure as well.

The optimum power allocation versus SNR value is shown more explicitly in Fig. 7. Moreover, this figure analyzes the effect of unequal noise level at the relays and destination. It is clearly seen that the communication hop with higher noise level requires higher share of the power pool, which is an expected observation.

The overall system end-to-end BER performance versus $E_b/N_0 = M\frac{SNR}{R_c}$ is presented in Fig. 8, where E_b is the total energy per information bit, N_0 is one sided noise power, M is the number of sensors and R_c is the coding rate at each sensor. To eliminate the flactuation effect in the BER curve, simulation is perfomed over extremely large number of frames. Dashed line in this figure shows the analytical probability of bit error based on equation (28) for *inner channels*, which matches the simulation results. The red line shows the upper bound on the overall system BER performance derived in equation (34). Simulation results show that the performance of *basic decoder* approaches the upper bound for high SNR values. The performance gap between the upper bound and the basic decoder is due to the approximations in deriving upper bound in equations (31) to (34). Moreover, in the upper bound calculations, for simplicity, we first calculate the source-to-

destination error probability for each sensor and then apply the majority vote on the resulting hard bits; while in the implementation of basic decoder, a hard limiter is applied directly on the summation of the soft outputs (LLRs) of the constituent decoders, which is more efficient.

It can be seen that the proposed iterative decoder outperforms the *basic decoder*. The performance improvement ranges from 1 to 4 dB for different SNR values. This improvement is due to considering observation model in the iterative decoding algorithm and using the average of other sensors' observations as side information in decoding a particular sensor's observation. However, the error floor of the overall system is not considerably improved since it is imposed by the number of sensors and observation error parameter as in (35).

Fig. 9 demonstrates the performance improvement gained by the proposed model employing two supernodes and utilizing D-STBC in a two-tiered network. This figure presents three setups for the inner channel including i) single super-node scenario ii) double super-node without STBC and iii) double super-node with STBC, all performing DMF relaying. The total power for all scenarios are equal to keep the comparison fair. It is shown that using two supernodes increases the performance by about $2 \sim 3$ dB due to the space diversity

gain. Also, about 1 dB additional gain is obtained using D-STBC due to the space-time diversity. All schemes ultimately reach the error floor for extremely large SNR values, which is corresponding to error-free communications as calculated in (35).

V. CONCLUSION

In this article, a two-tiered WSN system model is proposed to estimate an inaccessible binary data source using multiple observations. It was shown that the end-to-end system BER performance can be formulated as a function of the number of sensors inside each cluster, the observation accuracy, and the equivalent SNR value. As a thumbnail rule, higher number of sensors are needed to compensate lower observation accuracy, since the high error floor can not be compensated by improving the coding scheme. This provides an additional criterion for clustering algorithms to determine the minimum number of sensors in each cluster. This consideration minimizes the implementation and maintenance cost.

The idea of using two supernodes per cluster is proposed for this problem and D-STBC assisted DMF relaying is chosen as an appropriate near-optimal relaying scheme for this setup. This scheme provides the following advantages: (i) applicability to orthogonal channels in addition to common channels, (ii) no need for carrier-level synchronizations and (iii) facilitating the packet reformatting. Numerical results presents about 3 dB improvement in the end-to-end BER performance due to utilizing the proposed two-hop relaying method. This is in addition to about $1 \sim 4$ dB coding gain obtained by using PCCC based D-JSCC in the first tier, compare to the traditional basic coder, as discussed in Sec. IV.

Optimum power allocation is found by introducing the inner channel concept in order to optimize the system end-to-end BER performance. It is concluded that a higher share of available power should be assigned to the first tier (sensor nodes) in higher SNR regimes. This power optimization can be applied to any similar multiple-relaying system utilizing DMF relaying mode.

VI. ACKNOWLEDGMENT

REFERENCES

[1] T. Berger, Z. Zhang, and H. Viswanathan, "The CEO problem [multi-terminal source coding]," *IEEE Trans. Inf. Theory*, vol. 42, no. 3, May 1996.
[2] Y. Oohama, "The rate-distortion function for the quadratic Gaussian CEO problem," *IEEE Trans. Inf. Theory*, vol. 44, no. 3, pp. 1057–1070, May 1998.
[3] V. Prabhakaran, D. Tse, and K. Ramachandran, "Rate region of the quadratic Gaussian CEO problem," in *Proc. 2004 IEEE Int. Symp. Inf. Theory*, p. 119.
[4] J. Wang, J. Chen, and X. Wu, "On the sum rate of Gaussian multiter-minal source coding: new proofs and results," *IEEE Trans. Inf. Theory*, vol. 56, no. 8, pp. 3946–3960, Aug. 2010.
[5] Y. Yang and Z. Xiong, "On the generalized gaussian CEO problem," *IEEE Trans. Inf. Theory*, vol. 58, no. 6, pp. 3350–3372, June 2012.
[6] C. Jiang, D. Yuan, and Y. Zhao, "Towards clustering algorithms in wireless sensor networks-a survey," in *Proc. 2009 IEEE Wireless Commun. Netw. Conf.*, pp. 1–6.

[7] Z.-Y. Xiong, X.-P. Fan, S.-Q. Liu, and Z. Zhong, "Distributed image coding in wireless multimedia sensor networks: a survey," in *Proc. 2010 Advanced Computational Intelligence Workshop*, pp. 618–622.
[8] W. Bajwa, J. Haupt, A. Sayeed, and R. Nowak, "Joint source-channel communication for distributed estimation in sensor networks," *IEEE Trans. Inf. Theory*, vol. 53, no. 10, pp. 3629–3653, Oct. 2007.
[9] R. Maunder, J. Wang, S. Ng, L.-L. Yang, and L. Hanzo, "On the performance and complexity of irregular variable length codes for near-capacity joint source and channel coding," *IEEE Trans. Wireless Commun.*, vol. 7, no. 4, pp. 1338–1347, Apr. 2008.
[10] S. Pradhan and K. Ramchandran, "Distributed source coding using syndromes (discus): design and construction," in *Proc. 1999 Data Compression Conf.*, pp. 158–167.
[11] J. Bajcsy and P. Mitran, "Coding for the Slepian-Wolf problem with turbo codes," in *Proc. 2001 IEEE Global Telecommun. Conf.*, vol. 2, pp. 1400–1404.
[12] A. Liveris, Z. Xiong, and C. Georghiades, "Compression of binary sources with side information at the decoder using LDPC codes," *IEEE Commun. Lett.*, vol. 6, no. 10, pp. 440–442, Oct. 2002.
[13] A. Aaron and B. Girod, "Compression with side information using turbo codes," in *Proc. 2002 Data Compression Conf.*, pp. 252–261.
[14] J. Garcia-Frias and Z. Xiong, "Distributed source and joint source-channel coding: from theory to practice," in *Proc. 2005 IEEE Acoustics, Speech, and Signal Processing Conf.*, vol. 5, pp. 1093–1096.
[15] A. Razi, K. Yasami, and A. Abedi, "On minimum number of wireless sensors required for reliable binary source estimation," in *Proc. 2011 IEEE Wireless Commun. Netw. Conf.*, pp. 1852–1857.
[16] J. Harshan and B. Rajan, "Co-ordinate interleaved distributed space-time coding for two-antenna-relays networks," *IEEE Trans. Wireless Commun.*, vol. 8, no. 4, pp. 1783–1791, Apr. 2009.
[17] X. Guo and X.-G. Xia, "A distributed space-time coding in asynchronous wireless relay networks," *IEEE Trans. Wireless Commun.*, vol. 7, no. 5, pp. 1812–1816, May 2008.
[18] M. Kobayashi and X. Mestre, "Impact of CSI on distributed space-time coding in wireless relay networks," *IEEE Trans. Wireless Commun.*, vol. 8, no. 5, pp. 2580–2591, May 2009.
[19] J. Abouei, H. Bagheri, and A. Khandani, "An efficient adaptive distributed space-time coding scheme for cooperative relaying," *IEEE Trans. Wireless Commun.*, vol. 8, no. 10, pp. 4957–4962, Oct. 2009.
[20] G. Scutari and S. Barbarossa, "Distributed space-time coding for regenerative relay networks," *IEEE Trans. Wireless Commun.*, vol. 4, no. 5, pp. 2387–2399, Sept. 2005.
[21] Y. Jing and B. Hassibi, "Distributed space-time coding in wireless relay networks," *IEEE Trans. Wireless Commun.*, vol. 5, no. 12, pp. 3524–3536, Dec. 2006.
[22] B. Maham and S. Nader-Esfahani, "Performance analysis of distributed space-time codes in amplify-and-forward mode," in *Proc. 2007 IEEE Signal Process. Advances Wireless Commun. Workshop*, pp. 1–5.
[23] J. Kieffer, "Capacity of binary symmetric averaged channels," *IEEE Trans. Inf. Theory*, vol. 53, no. 1, pp. 288–303, Jan. 2007.
[24] Z. Krusevac, P. Rapajic, and R. Kennedy, "Concept of time varying binary symmetric model-channel uncertainty modeling," in *Proc. 2004 Int. Conf. Commun. Syst.*, pp. 598–602.
[25] J. Garcia-Frias and Y. Zhao, "Compression of binary memoryless sources using punctured turbo codes," *IEEE Commun. Lett.*, vol. 6, pp. 394–396, Sept. 2002.
[26] T. M. Cover and J. Thomas, *Elements of Information Theory*. Wiley, 1991.
[27] A. Nosratinia, "Relays and cooperative communication," in *Proc. 2010 IEEE Global Telecommun. Conf.*
[28] A. Razi, F. Afghah, and A. Abedi, "Binary source estimation using two-tiered sensor network," *IEEE Commun. Lett.*, vol. 5, no. 4, pp. 449–451, Apr. 2011.
[29] A. Dana and B. Hassibi, "On the power efficiency of sensory and ad hoc wireless networks," *IEEE Trans. Inf. Theory*, vol. 52, no. 7, pp. 2890–2914, July 2006.
[30] M. Gastpar and M. Vetterli, "On the capacity of wireless networks: the relay case," in *Proc. 2002 IEEE Int Conf. Comput. Commun.*, vol. 3, pp. 1577–1586.
[31] D. Tse and P. Viswanath, *Fundamentals of Wireless Commun.* Cambridge University Press, 2004.
[32] A. Lapidoth, "Near neighbour decoding for additive non-Gaussian noise channels," *IEEE Trans. Inf. Theory*, vol. 42, no. 5, pp. 1520–1529, Sept. 1996.
[33] S. Avestimehr and I. Shomorony, "Worst-case additive noise in wireless networks," arXiv:1208.1784, May 2012.
[34] F. Massey, "The Kolmogorov-Smirnov test for goodness of fit," *J. American Statistical Assoc.*, vol. 46, no. 253, pp. 68–78, Mar. 1951.

[35] G. Marsaglia, W. Tsang, and J. Wang, "Evaluating Kolmogorov's distribution," *J. Statistical Software*, vol. 8, no. 18, pp. 68–78, Nov. 2003.

[36] S. Lin and D. Costello, *Error Control Coding: Fundamentals and Applications*. Prentice Hall, 1983.

Abolfazl Razi received his B.Sc. and M.Sc. in Electrical Engineering from Sharif University of Technology and Amirkabir University of Technology, respectively. He is now pursuing his Ph.D in Electrical and Computer Engineering at University of Maine, Orono, ME. He is currently a visiting student at the ECE department, University of Maryland, College Park, MD. He is appointed as PACE chair of IEEE Maine Section, since January 2010. He was with Payam Noor University, Tehran from 2008 to 2009 as lecturer. He also served as project manager and R&D expert in several wireless companies including MCI, PTK, and FARDA. He was awarded the best graduate research assistant in 2011 and international graduate student scholarship in 2009 form University of Maine. He also received the best paper award from IEEE/CANEUS fly by wireless workshop, 2011. His research interests include distributed coding, multiuser communications, game theoretical optimizations and passive sensors.

Fatemeh Afghah is a PhD candidate at Electrical and Computer Engineering, University of Maine, Orono, USA. She is currently a visiting student at the ECE department, University of Maryland. She received the B.Sc. and M.Sc. degrees (both with honors) in Electrical Engineering from Khajeh Nassir Toosi University of Technology (K.N.T.U), Tehran, Iran in 2005 and 2008, respectively. Since Jan. 2011, she serves as GOLD chair at IEEE Maine Section. She was a Member-at-Large of IEEE Maine section (2010-11). From 2008 to 2009, she was with the FARDA Telecommunication company, Tehran. She is ITU youth fellow alumni from ITU Telecom World 2006, Hong Kong. She received several awards during her study such as MEIF Doctoral Fellowship Award, University of Maine, 2012, elite student award during the BSC and MSC form K.N.Toosi University. She also was granted Fellowship by ITU TELECOM world, 2008. Her researches focus on wireless communication systems, cooperation communication networks, relay channels, game theory, information theory and channel coding.

Ali Abedi received his B.Sc and M.Sc degrees in Electrical Engineering from Sharif University of Technology, and his Ph.D in Electrical and Computer Engineering from University of Waterloo in 1996, 1998, and 2004, respectively. He joined University of Maine in 2005, where he is currently Associate Professor of Electrical and Computer Engineering and Director of WiSe-Net Lab. Prior to joining the University of Maine, he was a lecturer at Queens University, and University of Waterloo. Dr. Abedi held Visiting Associate Professor position at the University of Maryland, College Park in 2012 and affiliate faculty position at Maine Institute for Human Genetics and Health from 2010-11.

Dr. Abedi has authored two books and over 60 research articles in Wireless Communications field. Highlights of his research include analytical performance evaluation of block codes, new methods for performance and convergence analysis of Turbo-codes, and applications of error correction codes in wireless sensor networks for structural monitoring, space explorations and biomedical engineering. His research on wireless sensing of lunar habitat was featured on NSF Science360 website in 2012. Dr. Abedi is a senior member of IEEE and candidate for IEEE Board of Directors in 2013 elections.